Kirchhoff prestack depth migration in orthorhombic velocity models with differently rotated tensors of elastic moduli

Václav Bucha
Department of Geophysics, Faculty of Mathematics and Physics, Charles University in Prague, Ke Karlovu 3, 121 16 Praha 2, Czech Republic, bucha@seis.karlov.mff.cuni.cz

Summary

We use the ray-based Kirchhoff prestack depth migration to calculate migrated sections in simple anisotropic homogeneous velocity models in order to show the impact of rotation of the tensor of elastic moduli on migrated images. The recorded wave field is generated in models composed of two homogeneous layers separated by a non-inclined curved interface. The anisotropy of the upper layer is orthorhombic with a differently rotated tensor of elastic moduli. We apply the Kirchhoff prestack depth migration to single-layer velocity models with orthorhombic anisotropy with and without the rotation of the tensor of elastic moduli. We show and discuss the errors of the migrated interface caused by incorrect velocity models used for migration. The study is limited to P-waves.

Keywords

3-D Kirchhoff prestack depth migration, anisotropic velocity model, rotation of the tensor of elastic moduli, orthorhombic anisotropy

1. Introduction

In this paper we extend the results presented in paper by Bucha (2013c) who rotated the tensor of elastic moduli around the axis x_2 only. The extension includes rotations around axes x_1 and x_3.

The dimensions of the velocity model, shot-receiver configuration, methods for calculation of the recorded wave field and the migration are the same as in the previous papers by Bucha (2011, 2012a, 2012b, 2013a, 2013b, 2013c). Our aim is to study the effect of the rotation of the tensor of elastic moduli in models with orthorhombic anisotropy on migrated images.

To compute the synthetic recorded wave field, we use simple anisotropic velocity models composed of two homogeneous layers separated by one curved interface that is non-inclined in the direction perpendicular to the source-receiver profiles. The anisotropy in the upper layer is orthorhombic with the rotation of the tensor of elastic moduli. The angles of rotation are equal to 15, 30 and 45 degrees around axes x_1, x_2 or x_3, respectively.

We migrate in correct and incorrect single-layer orthorhombic velocity models with and without the rotation of the elasticity tensor. The distribution of elastic moduli in each correct model corresponds to the upper layer of the velocity model in which the corresponding synthetic data have been calculated. Incorrect models have orthorhombic anisotropy without the rotation of the tensor of elastic moduli.

Seismic Waves in Complex 3–D Structures, **24** (2014), 59–75 (ISSN 2336–3827, online at http://sw3d.cz)

We show mispositioning and defocusing of the migrated interface caused by incorrect velocity models used for migration. The calculations are limited to P-waves.

2. Anisotropic velocity models

The dimensions of the velocity models and measurement configurations are derived from the 2-D Marmousi model and dataset (Versteeg & Grau, 1991). The horizontal dimensions of the velocity model are $0\ km \leq x_1 \leq 9.2\ km$, $0\ km \leq x_2 \leq 10\ km$ and the depth is $0\ km \leq x_3 \leq 3\ km$. The velocity model is composed of two layers separated by one non-inclined curved interface (see Figure 1). The curved interface is non-inclined in the direction of the x_2 axis which is perpendicular to the source-receiver profiles.

2.1 Velocity models for the recorded wave field

The recorded wave field is computed in the velocity models composed of two layers. The medium in the upper layer of these velocity models is orthorhombic (Schoenberg & Helbig, 1997). The medium is vertically fractured and is composed of two elements. The first element is a transversely isotropic background medium with a vertical axis of symmetry. The second element is a set of parallel vertical fractures.

We use nine velocity models with the orthorhombic anisotropy with differently rotated tensors of elastic moduli in the upper layer (see Figure 1). The angles of the rotation are 15, 30 and 45 degrees around axes x_1 (Section 2.1.1), x_2 (Section 2.1.2) or x_3 (Section 2.1.3).

The bottom layer in all nine velocity models is isotropic and the P-wave velocity in the layer is $V_p = 3.6\ km/s$. The S-wave velocity is $V_s = V_p/\sqrt{3}$.

2.1.1 Orthorhombic anisotropy with the rotation around axis X1

The matrix of density-reduced elastic moduli A_{ij} in km^2/s^2 for the rotation angle around axis x_1 equal to

a) 15 degrees (OA-X1-15) reads

$$\begin{pmatrix} 9.00 & 3.51 & 2.34 & 0.34 & 0.00 & 0.00 \\ & 9.39 & 2.59 & 0.81 & 0.00 & 0.00 \\ & & 6.01 & 0.17 & 0.00 & 0.00 \\ & & & 2.19 & 0.00 & 0.00 \\ & & & & 1.64 & 0.15 \\ & & & & & 2.14 \end{pmatrix}, \tag{1a}$$

b) 30 degrees (OA-X1-30) reads

$$\begin{pmatrix} 9.00 & 3.26 & 2.59 & 0.58 & 0.00 & 0.00 \\ & 8.31 & 2.96 & 1.17 & 0.00 & 0.00 \\ & & 6.35 & 0.52 & 0.00 & 0.00 \\ & & & 2.56 & 0.00 & 0.00 \\ & & & & 1.75 & 0.25 \\ & & & & & 2.04 \end{pmatrix}, \tag{1b}$$

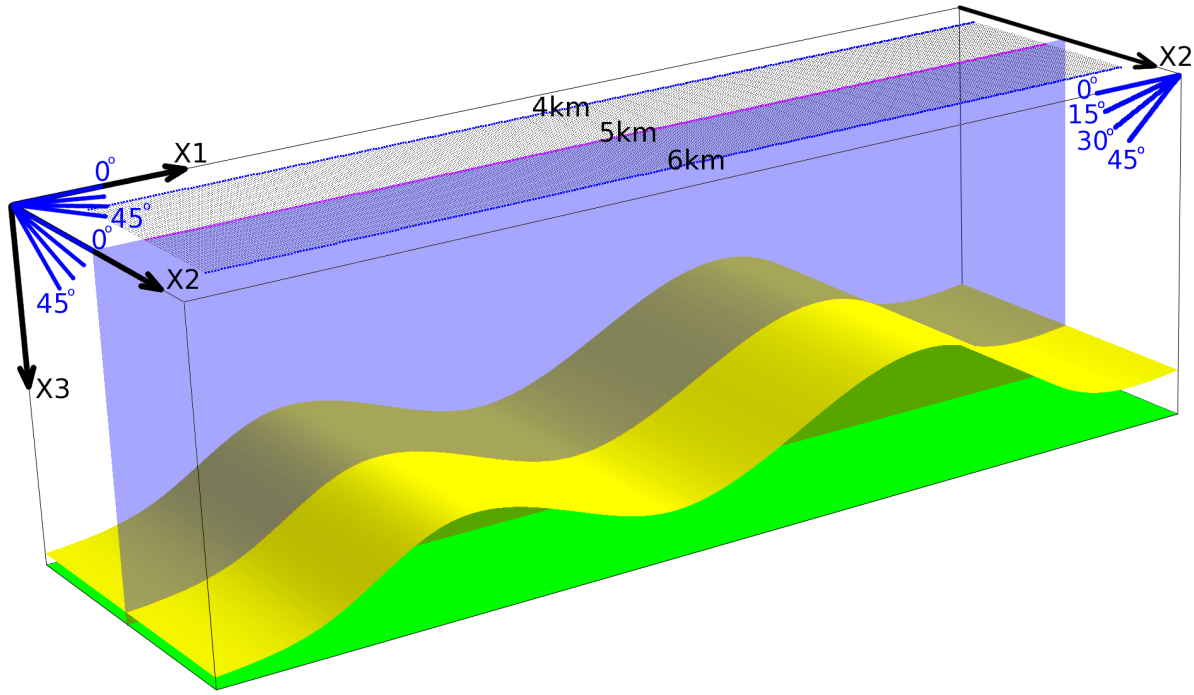

Figure 1. Part of the velocity model with 81 parallel profile lines, the non-inclined curved interface and the bottom velocity model plane. The horizontal dimensions of the depicted part of the velocity model are 0 $km \leq x_1 \leq 9.2$ km, 3.5 $km \leq x_2 \leq 6.5$ km, the depth is 0 $km \leq x_3 \leq 3$ km. We compute and stack migrated sections in the 2-D plane located in the middle of the shot-receiver configuration, at horizontal coordinate $x_2 = 5$ km. The rotation of the tensor of elastic moduli around axes x_1, x_2 or x_3 is equal to 15, 30 and 45 degrees.

c) 45 degrees (OA-X1-45) reads

$$\begin{pmatrix} 9.00 & 2.93 & 2.93 & 0.68 & 0.00 & 0.00 \\ & 7.14 & 3.14 & 0.98 & 0.00 & 0.00 \\ & & 7.14 & 0.98 & 0.00 & 0.00 \\ & & & 2.74 & 0.00 & 0.00 \\ & & & & 1.89 & 0.29 \\ & & & & & 1.89 \end{pmatrix}. \tag{1c}$$

2.1.2 Orthorhombic anisotropy with the rotation around axis X2

The matrix of density-reduced elastic moduli A_{ij} in km^2/s^2 for the rotation angle around axis x_2 equal to

a) 15 degrees (OA-X2-15) reads

$$\begin{pmatrix} 8.54 & 3.52 & 2.50 & 0.00 & -0.82 & 0.00 \\ & 9.84 & 2.48 & 0.00 & -0.30 & 0.00 \\ & & 5.89 & 0.00 & 0.05 & 0.00 \\ & & & 2.01 & 0.00 & -0.05 \\ & & & & 1.85 & 0.00 \\ & & & & & 2.17 \end{pmatrix}, \tag{2a}$$

b) 30 degrees (OA-X2-30) reads

$$\begin{pmatrix} 7.48 & 3.30 & 3.01 & 0.00 & -1.10 & 0.00 \\ & 9.84 & 2.70 & 0.00 & -0.52 & 0.00 \\ & & 5.95 & 0.00 & -0.23 & 0.00 \\ & & & 2.05 & 0.00 & -0.08 \\ & & & & 2.36 & 0.00 \\ & & & & & 2.14 \end{pmatrix}, \tag{2b}$$

c) 45 degrees (OA-X2-45) reads

$$\begin{pmatrix} 6.46 & 3.00 & 3.26 & 0.00 & -0.77 & 0.00 \\ & 9.84 & 3.00 & 0.00 & -0.60 & 0.00 \\ & & 6.46 & 0.00 & -0.77 & 0.00 \\ & & & 2.09 & 0.00 & -0.09 \\ & & & & 2.61 & 0.00 \\ & & & & & 2.09 \end{pmatrix}. \tag{2c}$$

2.1.3 Orthorhombic anisotropy with the rotation around axis X3

The matrix of density-reduced elastic moduli A_{ij} in km^2/s^2 for the rotation angle around axis x_3 equal to

a) 15 degrees (OA-X3-15) reads

$$\begin{pmatrix} 8.87 & 3.78 & 2.26 & 0.00 & 0.00 & 0.21 \\ & 9.60 & 2.39 & 0.00 & 0.00 & -0.42 \\ & & 5.94 & 0.00 & 0.00 & -0.04 \\ & & & 1.97 & -0.10 & 0.00 \\ & & & & 1.63 & 0.00 \\ & & & & & 2.36 \end{pmatrix}, \tag{3a}$$

b) 30 degrees (OA-X3-30) reads

$$\begin{pmatrix} 8.66 & 4.15 & 2.29 & 0.00 & 0.00 & 0.13 \\ & 9.08 & 2.36 & 0.00 & 0.00 & -0.50 \\ & & 5.94 & 0.00 & 0.00 & -0.06 \\ & & & 1.90 & -0.17 & 0.00 \\ & & & & 1.70 & 0.00 \\ & & & & & 2.73 \end{pmatrix}, \tag{3b}$$

c) 45 degrees (OA-X3-45) reads

$$\begin{pmatrix} 8.69 & 4.33 & 2.33 & 0.00 & 0.00 & -0.21 \\ & 8.69 & 2.33 & 0.00 & 0.00 & -0.21 \\ & & 5.94 & 0.00 & 0.00 & -0.08 \\ & & & 1.80 & -0.20 & 0.00 \\ & & & & 1.80 & 0.00 \\ & & & & & 2.91 \end{pmatrix}. \tag{3c}$$

2.2 Velocity models for the migration

We migrate in correct single-layer velocity models with orthorhombic anisotropy with the correctly rotated tensors of elastic moduli given by matrices (1a)–(3c). The distribution of elastic moduli in correct models corresponds to the upper layer of the velocity models in which the synthetic data have been calculated.

Additionally we migrate in incorrect single-layer velocity models with orthorhombic anisotropy without the rotation of the tensor of elastic moduli in order to simulate situations in which we have made an incorrect guess of the anisotropic velocity model for migration.

Orthorhombic anisotropy without the rotation (OA) is specified by Schoenberg & Helbig (1997). The matrix of density-reduced elastic moduli in km^2/s^2 reads

$$\begin{pmatrix} 9.00 & 3.60 & 2.25 & 0.00 & 0.00 & 0.00 \\ & 9.84 & 2.40 & 0.00 & 0.00 & 0.00 \\ & & 5.94 & 0.00 & 0.00 & 0.00 \\ & & & 2.00 & 0.00 & 0.00 \\ & & & & 1.60 & 0.00 \\ & & & & & 2.18 \end{pmatrix}. \tag{4}$$

3. Shots and receivers

The measurement configuration is derived from the Marmousi model and dataset (Versteeg & Grau, 1991). The profile lines are parallel with the x_1 coordinate axis. Each profile line has the following configuration: The first shot is 3 km from the left-hand side of the velocity model, the last shot is 8.975 km from the left-hand side of the velocity model, the distance between the shots is 0.025 km, and the depth of the shots is 0 km. The total number of shots along one profile line is 240. The number of receivers per shot is 96, the first receiver is located 2.575 km left of the shot location, the last receiver is 0.2 km left of the shot location, the distance between the receivers is 0.025 km, and the depth of the receivers is 0 km. This configuration simulates a simplified towed streamed acquisition geometry.

The 3-D measurement configuration consists of 81 parallel profile lines, see Figure 1. The distance between the parallel profile lines is 0.025 km.

4. Recorded wave field

The recorded wave field in the orthorhombic velocity models with the rotation of the tensor of elastic moduli was computed using the ANRAY software package (Gajewski & Pšenčík, 1990). 3-D ray tracing is used to calculate the two-point rays of the reflected P-wave. We then compute the ray-theory seismograms at the receivers.

The two-point rays do not stay in the vertical planes corresponding to the individual profiles. Figures 2–6 show the deflection of two-point rays from the vertical plane for selected profile line and selected shot-receiver configurations. The deflection is the smallest for rotations of the elasticity tensor around coordinate axis x_2.

The recorded wave field is equal for all parallel profile lines, because the distribution of elastic moduli is 1-D and the non-inclined curved interface is independent of the coordinate x_2 perpendicular to the profile lines (2.5-D velocity model, see Figure 1).

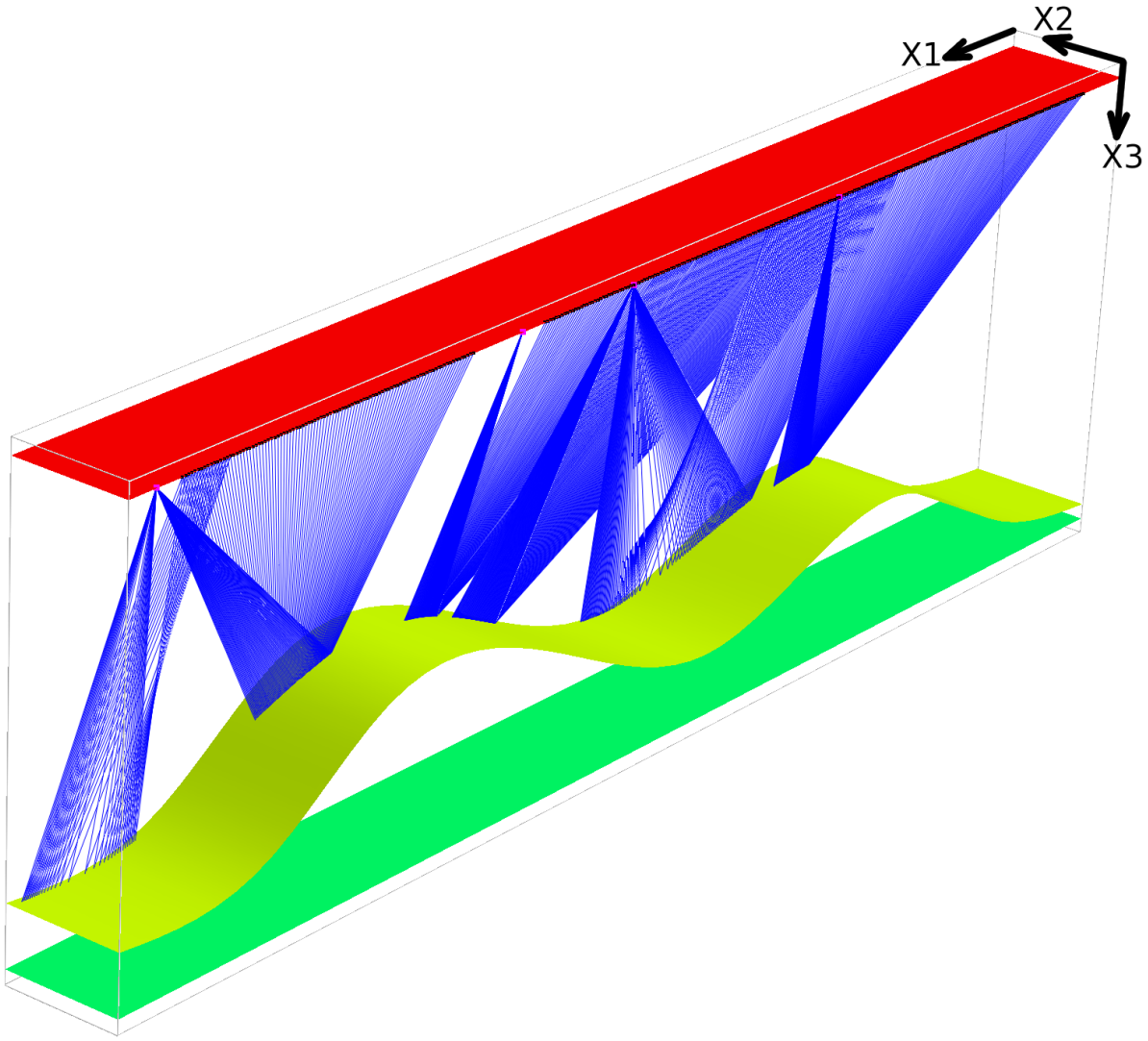

Figure 2. Two-point rays of the reflected P-wave for one selected profile line (at horizontal coordinate $x_2 = 5\ km$) and four shot-receiver configurations (from the right-hand side shots 1, 80, 120 and 240 along the profile) are calculated in the velocity model with orthorhombic anisotropy rotated by 45 degrees around coordinate axis x_1 (OA-X1-45 medium). Note that the two-point rays do not stay in the vertical plane corresponding to the profile line. The profile line is situated at top edge of the depicted part of the model (black dots). The maximum deviation of reflections at the non-inclined curved interface is 0.80 km from vertical plane. The horizontal dimensions of the depicted part of the velocity model are 0 $km \leq x_1 \leq 9.2\ km$, 5.00 $km \leq x_2 \leq 5.80\ km$, the depth is 0 $km \leq x_3 \leq 3\ km$.

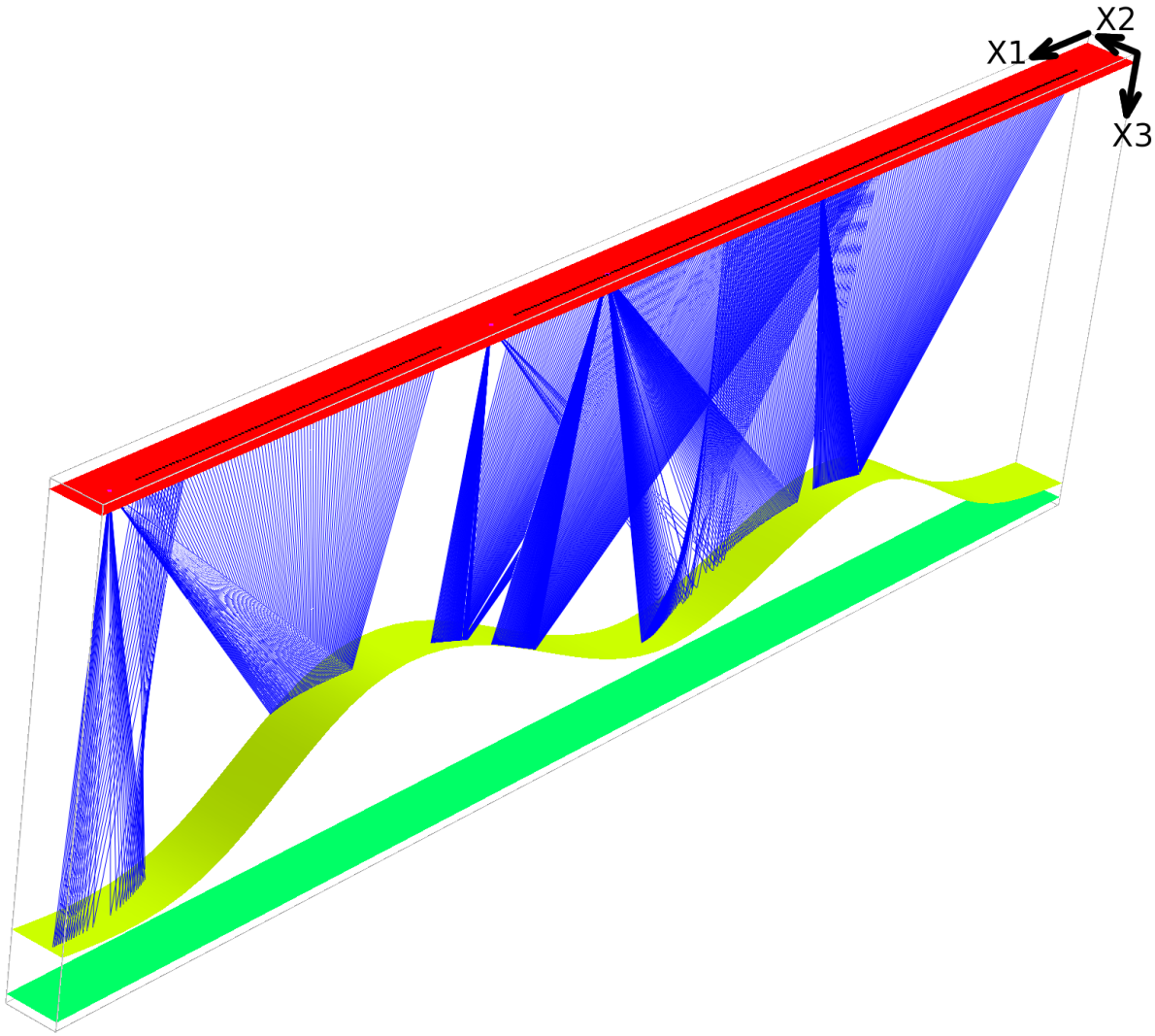

Figure 3. Two-point rays of the reflected P-wave for one selected profile line (at horizontal coordinate $x_2 = 5\ km$) and four shot-receiver configurations (from the right-hand side shots 1, 80, 120 and 240 along the profile) are calculated in the velocity model with orthorhombic anisotropy rotated by 45 degrees around coordinate axis x_3 (OA-X3-45 medium). Note that the two-point rays do not stay in the vertical plane corresponding to the profile line (black dots). The width of the non-inclined curved interface in the direction perpendicular to the profile line is 0.35 km. The horizontal dimensions of the depicted part of the velocity model are $0\ km \leq x_1 \leq 9.2\ km$, $4.85\ km \leq x_2 \leq 5.20\ km$, the depth is $0\ km \leq x_3 \leq 3\ km$.

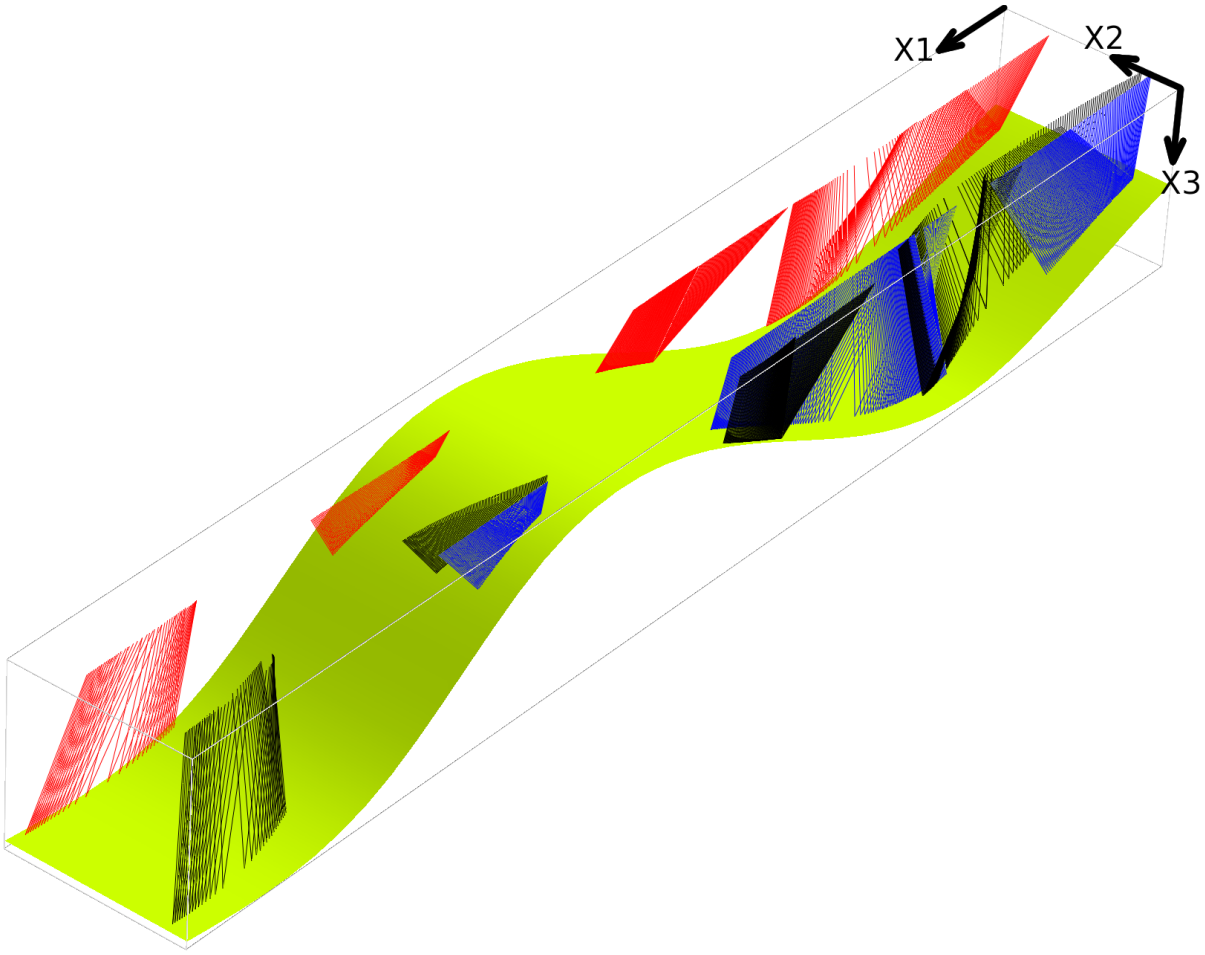

Figure 4. Detailed view of the bottom segments of two-point rays of the reflected P-wave for two shot-receiver configurations (from the right-hand side shots 80 and 240, profile line at $x_2 = 5\ km$). Two-point rays are calculated in three different velocity models with differently rotated orthorhombic anisotropy. The rays of three calculations are displayed together. **Red** two-point rays correspond to the rotation 45 degrees around coordinate axis x_1 (OA-X1-45 medium), **blue** two-point rays correspond to the rotation 45 degrees around coordinate axis x_2 (OA-X2-45 medium) and **black** two-point rays correspond to the rotation 45 degrees around coordinate axis x_3 (OA-X3-45 medium). The width of the interface in the direction perpendicular to the profile line is 0.95 km (4.85 $km \leq x_2 \leq 5.80\ km$). Note the different paths of reflections at the interface.

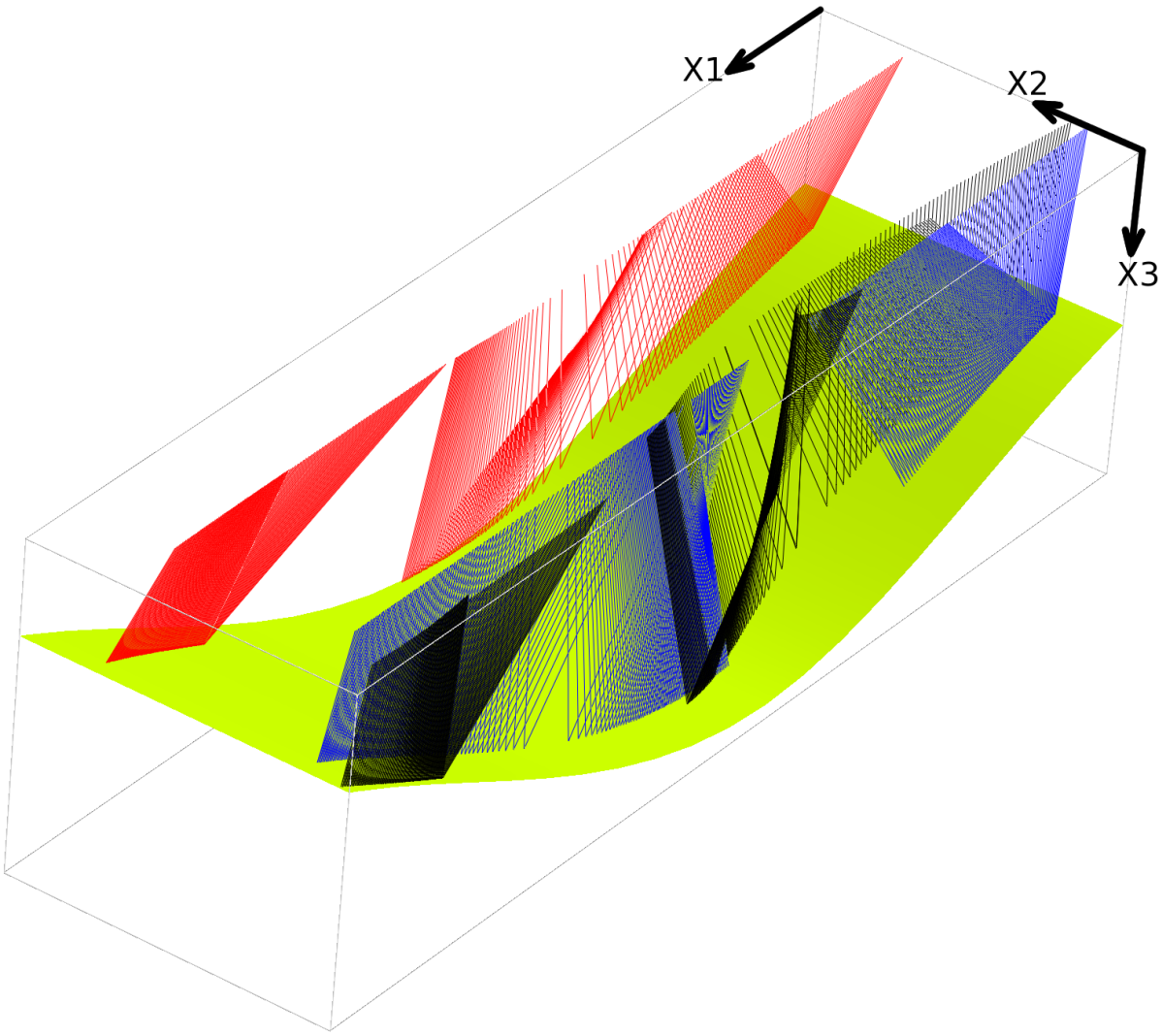

Figure 5. Detailed view of the bottom segments of two-point rays of the reflected P-wave for one shot-receiver configuration (shot 80, profile line at $x_2 = 5$ km). Two-point rays are calculated in three different velocity models with differently rotated orthorhombic anisotropy. The rays of three calculations are displayed together. **Red** two-point rays correspond to the rotation 45 degrees around coordinate axis x_1 (OA-X1-45 medium), **blue** two-point rays correspond to the rotation 45 degrees around coordinate axis x_2 (OA-X2-45 medium) and **black** two-point rays correspond to the rotation 45 degrees around coordinate axis x_3 (OA-X3-45 medium). The width of the interface in the direction perpendicular to the profile line is 0.95 km (4.85 $km \leq x_2 \leq 5.80$ km). Note the different paths of reflections at the interface.

5. Kirchhoff prestack depth migration

We use the MODEL, CRT, FORMS and DATA packages for the 3-D Kirchhoff prestack depth migration (Červený, Klimeš & Pšenčík, 1988; Bulant, 1996). The migration consists of two-parametric ray tracing from the individual surface points, calculating grid values of travel times and amplitudes, performing the common-shot migration and stacking the migrated images. The shot-receiver configuration consists of 81 parallel profile lines at intervals of 0.025 km (see Figure 1). The first profile line is situated at horizontal coordinate $x_2 = 4$ km and the last profile line is situated at horizontal coordinate $x_2 = 6$ km. For migration we use single-layer velocity models (without the curved interface).

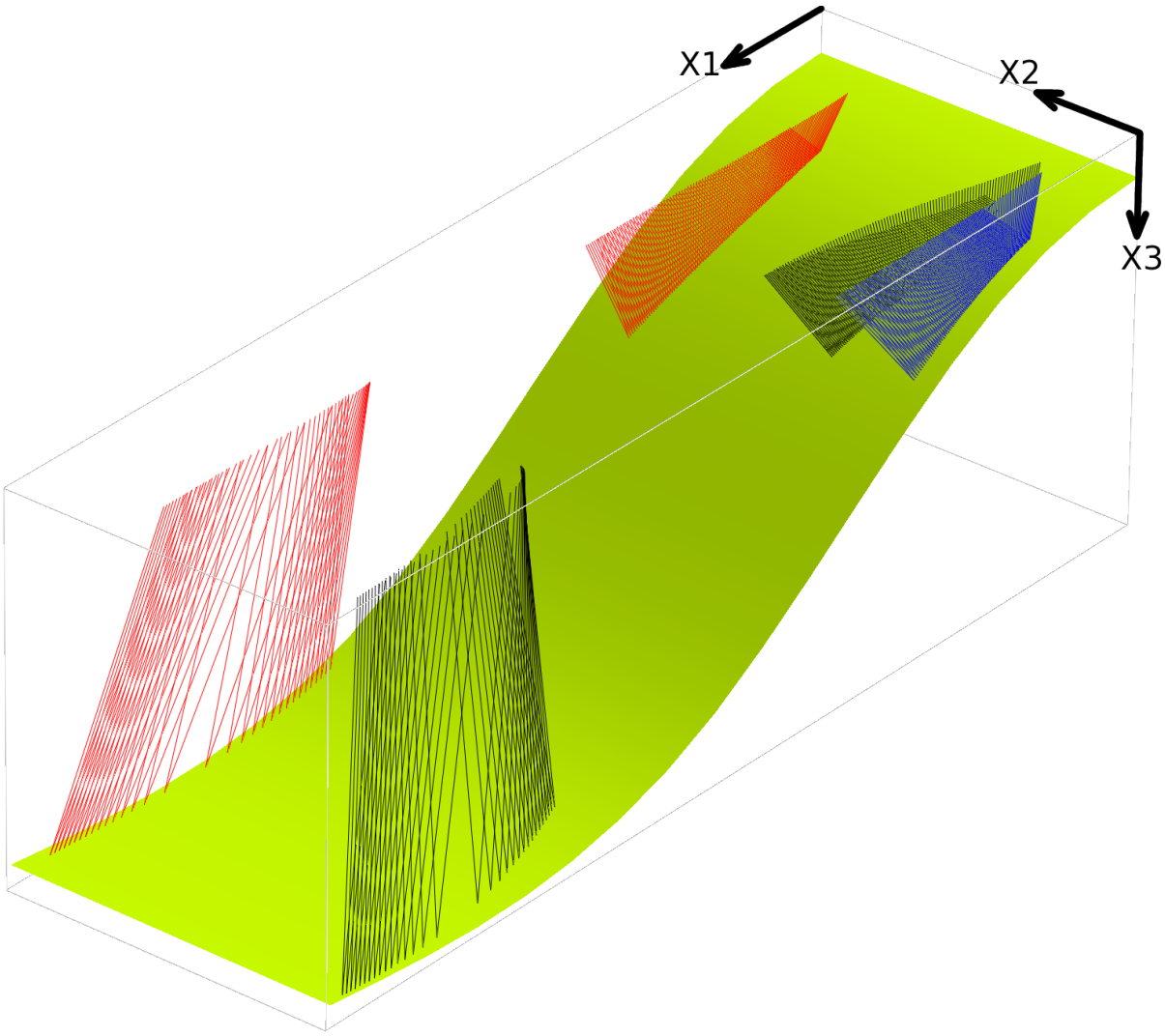

Figure 6. Detailed view of the bottom segments of two-point rays of the reflected P-wave for one shot-receiver configuration (shot 240, profile line at $x_2 = 5\ km$). Two-point rays are calculated in three different velocity models with differently rotated orthorhombic anisotropy. The rays of three calculations are displayed together. **Red** two-point rays correspond to the rotation 45 degrees around coordinate axis x_1 (OA-X1-45 medium), **blue** two-point rays correspond to the rotation 45 degrees around coordinate axis x_2 (OA-X2-45 medium) and **black** two-point rays correspond to the rotation 45 degrees around coordinate axis x_3 (OA-X3-45 medium). The width of the interface in the direction perpendicular to the profile line is 0.95 km (4.85 $km \leq x_2 \leq 5.80\ km$). Note the different paths of reflections at the interface.

We calculate only one vertical image section corresponding to the central profile line ($x_2 = 5\ km$, see Figure 1) and the image represents one vertical section of full 3-D migrated volume. We form the image by computing and summing the corresponding contributions (images) from all 81 parallel source-receiver lines. While summing the contributions, the constructive interference focuses the migrated interface and the destructive interference reduces undesirable migration artifacts (non-specular reflections). We also use a cosine taper to clear some residua.

5.1 Migration using the correct velocity models

The distribution of elastic moduli in the single-layer velocity model for migration is the same as the distribution in the upper layer of the velocity model used to calculate the recorded wave field (matrices (1a)–(3c)).

Figure 7 shows three stacked migrated sections calculated in the correct single-layer velocity models with the orthorhombic anisotropy with the rotation of the tensor of elastic moduli around axes x_1, x_2 or x_3 for angle 45 degrees. Migrated sections for angles of rotation 15 and 30 degrees are similar and we do not display them. The migrated interface is clear and coincides nearly perfectly with the interface in the velocity model used to compute the recorded wave field.

5.2 Migration using the incorrect velocity models

In this test, we use the Kirchhoff prestack depth migration to calculate migrated sections in incorrect homogeneous velocity models. We simulate situations in which we have made an incorrect guess of the rotation of the tensor of elastic moduli around axes x_1, x_2 or x_3. So we migrate in incorrect single-layer velocity models with orthorhombic anisotropy without the rotation of the tensor of elastic moduli defined by matrix (4) (OA medium).

Figure 8 shows three stacked migrated sections for the recorded wave field calculated in models with the orthorhombic anisotropy with the rotation of the tensor of elastic moduli around axis x_1 in the upper layer. The angles of rotation are 15, 30 and 45 degrees (matrices (1a), (1b) and (1c)). The migrated interface is shifted vertically upwards (undermigrated) and the shift increases with the angle of the rotation. This fact indicates that the models with rotated elasticity tensors are faster for reflected P-wave than models without rotation (matrix (4)). Note that the two-point rays are considerably deflected from the vertical plane corresponding to the profile line (see Figure 2). The angle of deflection increases with the angle of the rotation.

Results of the migration in models with the rotation around axis x_2 were presented already last year (Bucha, 2013c). The errors of the migrated interface increase with the angle of the rotation (see Figure 9). Note the nearly correctly migrated interface in the horizontal range of approximately $4-6$ km for all angles of the rotation. So the velocity of reflected P-waves for this part of the interface in models with rotated elasticity tensor is nearly the same as the velocity in the model without the rotation. The segments of the interface in horizontal ranges of approximately $2-4$ km and $6-8$ km are defocused and mispositioned (undermigrated), i.e. the velocity of reflected P-waves in models with rotated elasticity tensor is greater than the velocity in the model without the rotation (matrix (4)). Surprisingly the two-point rays in this case stay nearly in the vertical plane corresponding to the profile line.

Figure 10 shows three stacked migrated sections for the recorded wave field calculated in models with the orthorhombic anisotropy with the rotation of the tensor of elastic moduli around axis x_3 in the upper layer. The angles of rotation are 15, 30 and 45 degrees (matrices (3a), (3b) and (3c)). The migrated interface is slightly shifted vertically upwards (undermigrated). The shift increases with the angle of the rotation and is noticeable for the angle 45 degrees. Note that the two-point rays do not stay in the vertical plane corresponding to the profile line (see Figure 3).

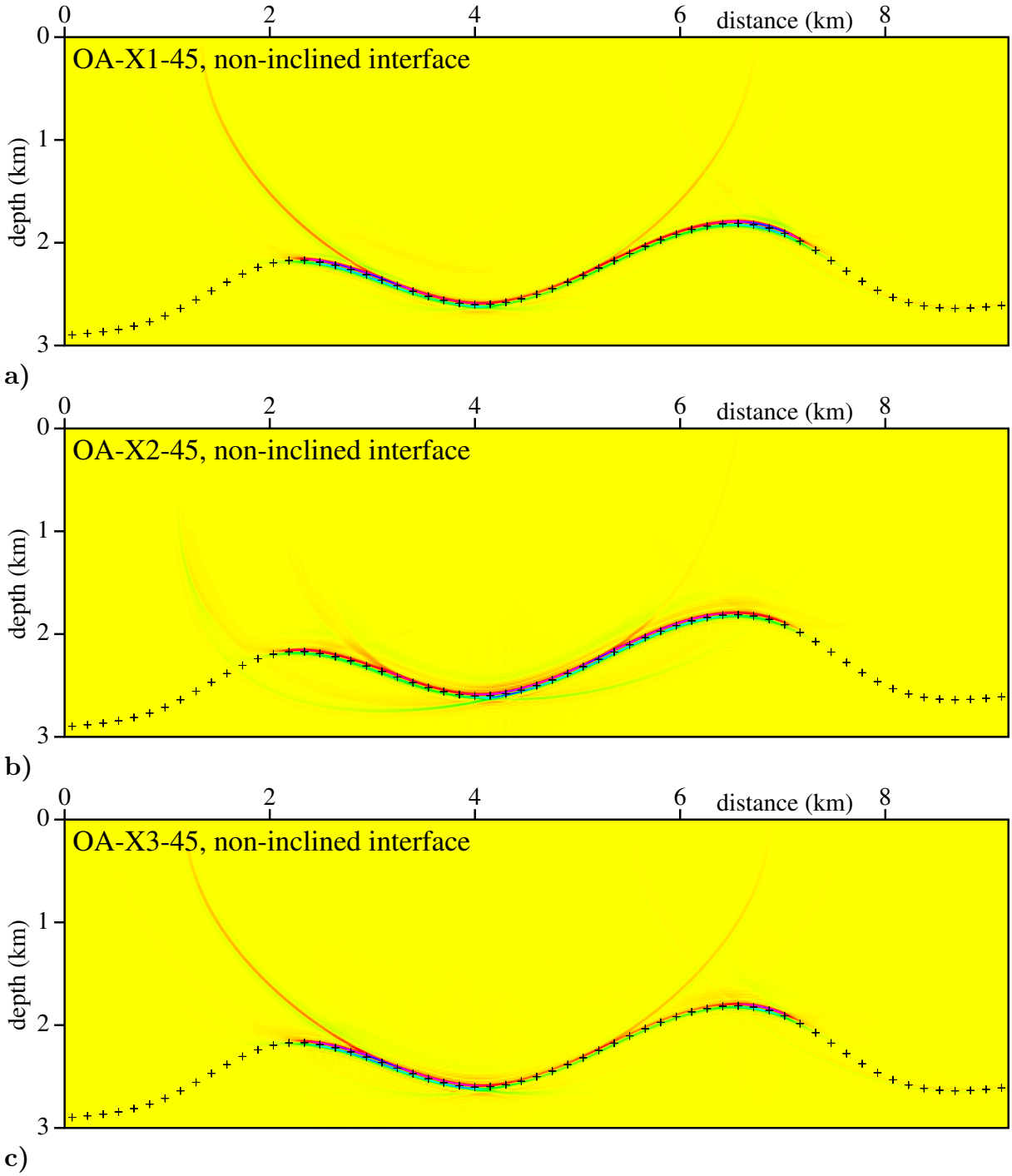

Figure 7. Stacked migrated sections calculated in the correct velocity models without interfaces, specified by orthorhombic anisotropy with **a)** 45 degree rotation of the tensor of elastic moduli around the x_1 axis (OA-X1-45), **b)** 45 degree rotation of the tensor of elastic moduli around the x_2 axis (OA-X2-45) and **c)** 45 degree rotation of the tensor of elastic moduli around the x_3 axis (OA-X3-45). The distribution of elastic moduli in the single-layer velocity models for migration is the same as the distribution in the upper layer of the velocity models used to calculate the recorded wave field. 81×240 common-shot prestack depth migrated sections, corresponding to 81 profile lines and 240 sources along each profile line, have been stacked. The crosses denote the interface in the velocity models used to compute the recorded wave field.

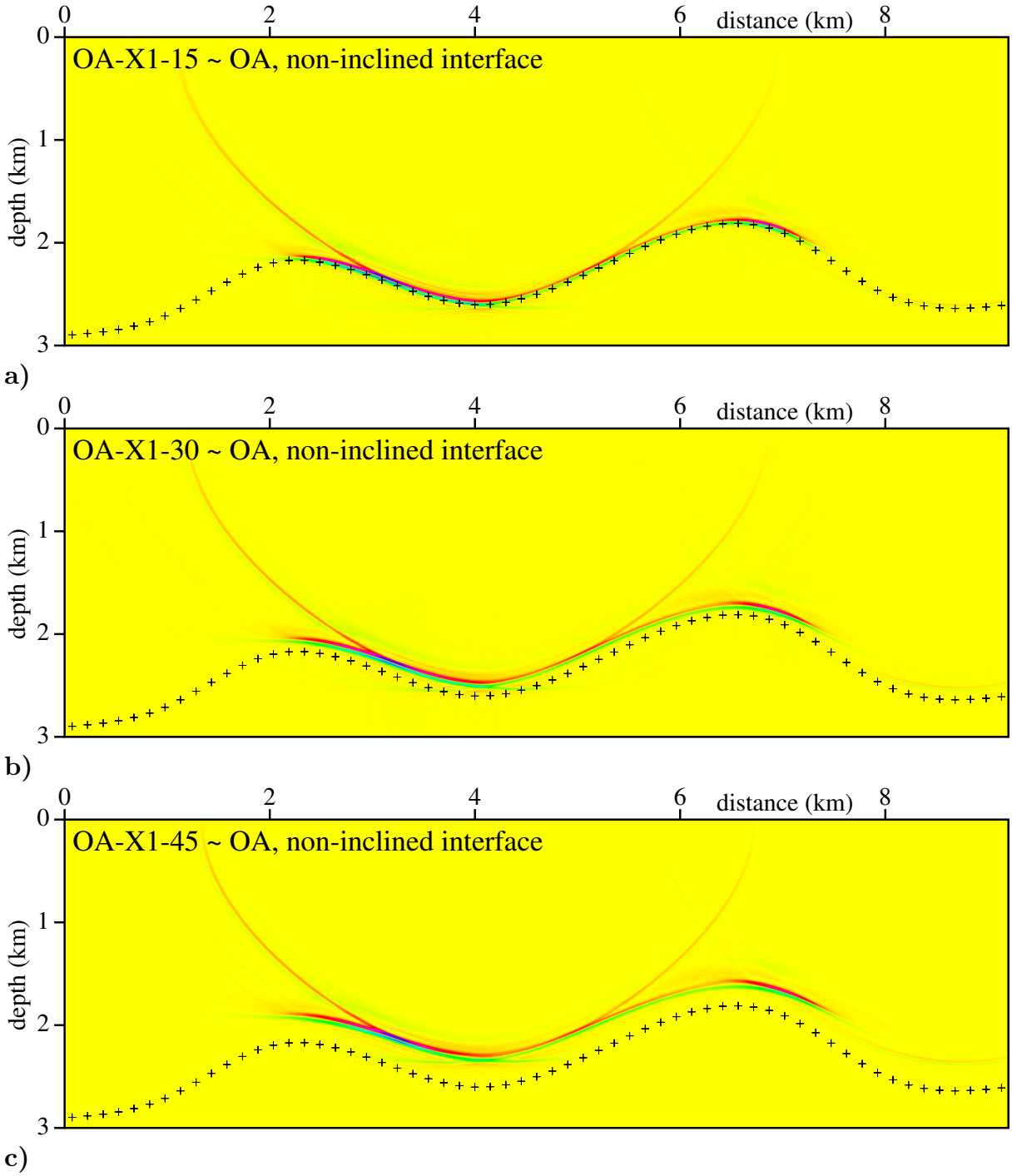

Figure 8. Stacked migrated sections calculated in the incorrect velocity models with orthorhombic anisotropy (OA) without the rotation of the tensor of elastic moduli. The correct anisotropy is orthorhombic with **a)** 15 degree rotation of the tensor of elastic moduli around the x_1 axis (OA-X1-15), **b)** 30 degree rotation of the tensor of elastic moduli around the x_1 axis (OA-X1-30) and **c)** 45 degree rotation of the tensor of elastic moduli around the x_1 axis (OA-X1-45). 81×240 common-shot prestack depth migrated sections, corresponding to 81 profile lines and 240 sources along each profile line, have been stacked. The crosses denote the interface in the velocity models used to compute the recorded wave field.

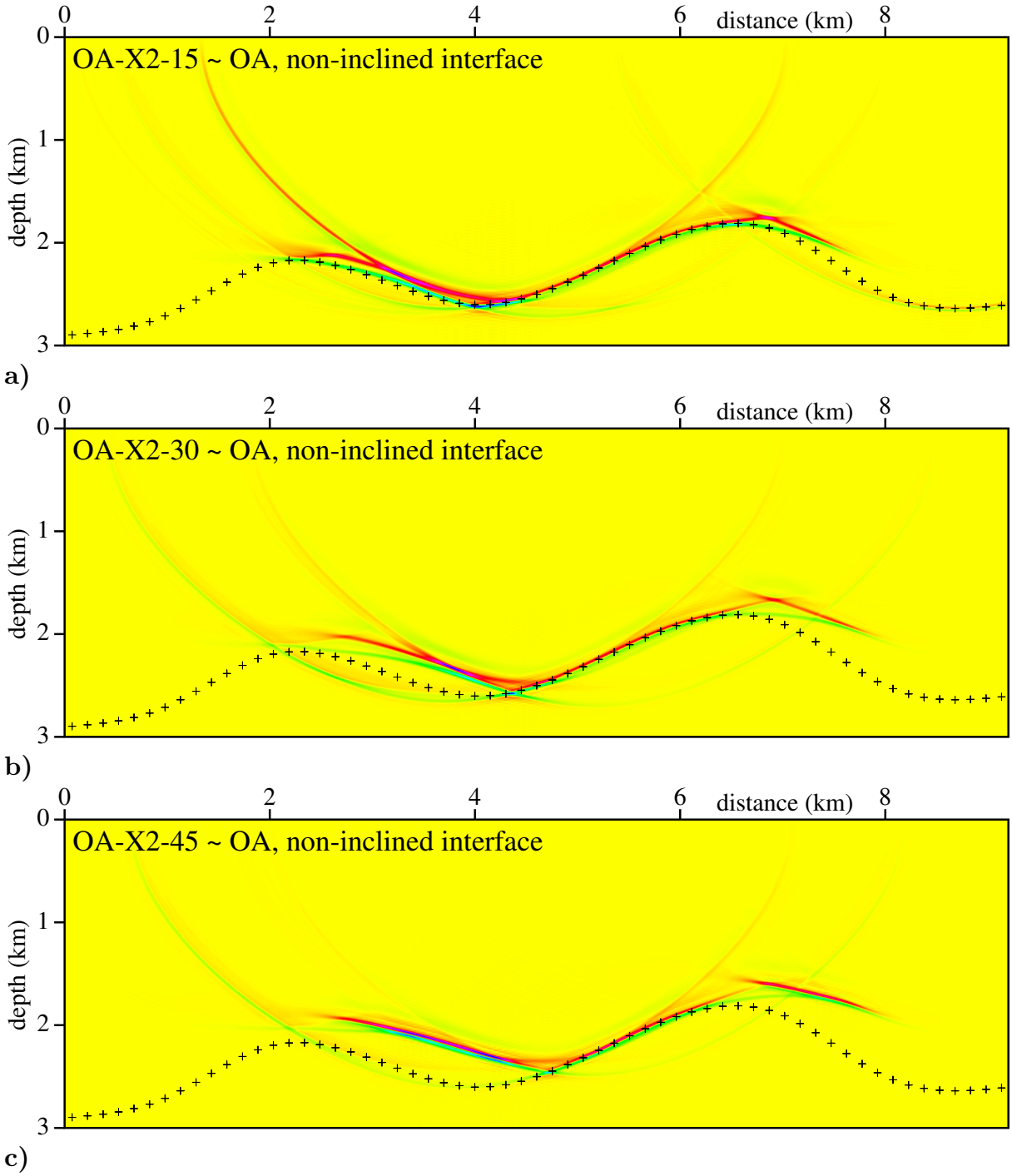

Figure 9. Stacked migrated sections calculated in the incorrect velocity models with orthorhombic anisotropy (OA) without the rotation of the tensor of elastic moduli. The correct anisotropy is orthorhombic with **a)** 15 degree rotation of the tensor of elastic moduli around the x_2 axis (OA-X2-15), **b)** 30 degree rotation of the tensor of elastic moduli around the x_2 axis (OA-X2-30) and **c)** 45 degree rotation of the tensor of elastic moduli around the x_2 axis (OA-X2-45). 81×240 common-shot prestack depth migrated sections, corresponding to 81 profile lines and 240 sources along each profile line, have been stacked. The crosses denote the interface in the velocity models used to compute the recorded wave field.

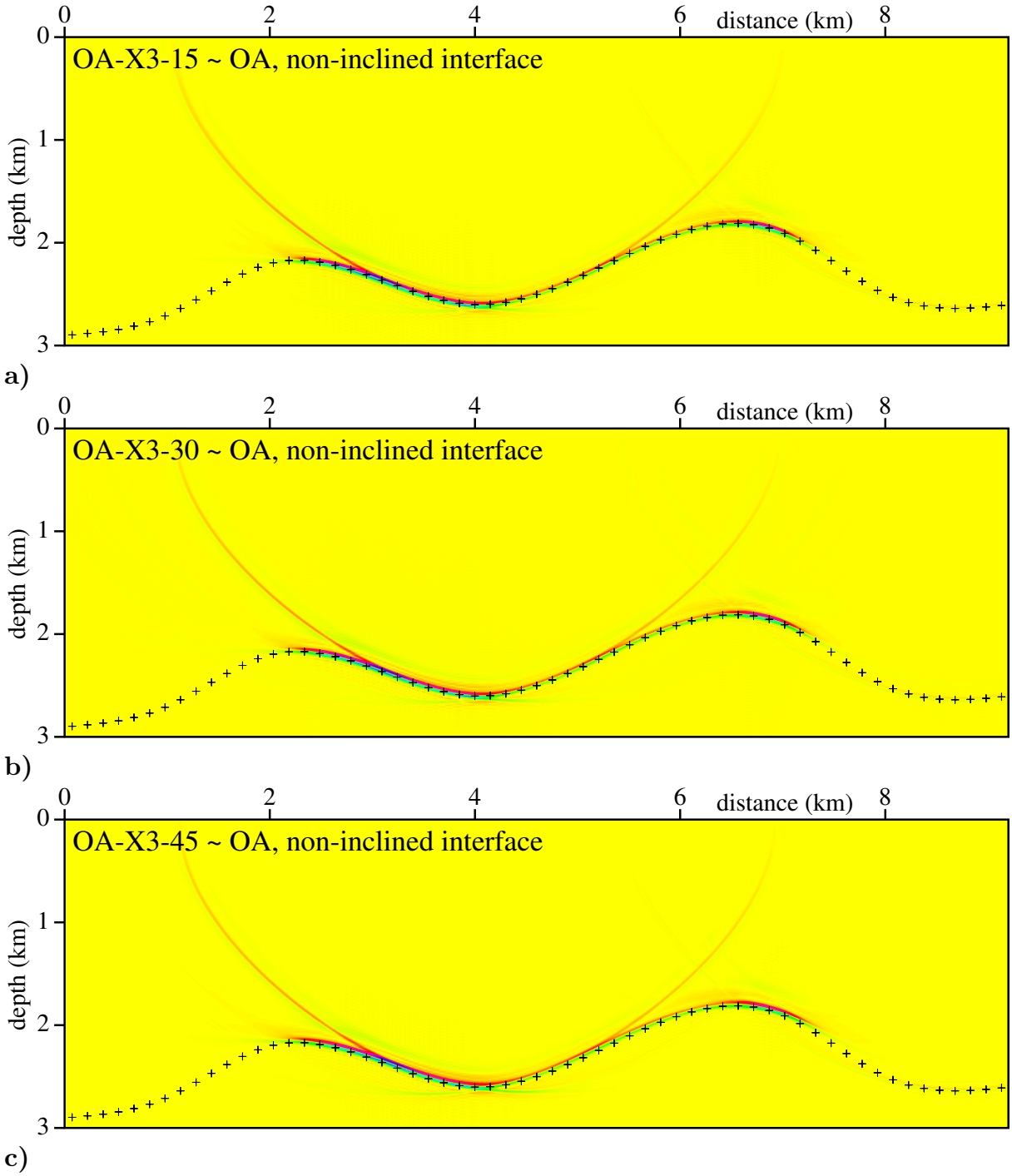

Figure 10. Stacked migrated sections calculated in the incorrect velocity models with orthorhombic anisotropy (OA) without the rotation of the tensor of elastic moduli. The correct anisotropy is orthorhombic with **a)** 15 degree rotation of the tensor of elastic moduli around the x_3 axis (OA-X3-15), **b)** 30 degree rotation of the tensor of elastic moduli around the x_3 axis (OA-X3-30) and **c)** 45 degree rotation of the tensor of elastic moduli around the x_3 axis (OA-X3-45). 81×240 common-shot prestack depth migrated sections, corresponding to 81 profile lines and 240 sources along each profile line, have been stacked. The crosses denote the interface in the velocity models used to compute the recorded wave field.

6. Conclusions

We generated synthetic seismograms using the ray theory in two-layer velocity models with orthorhombic anisotropy with differently rotated tensors of elastic moduli. Then we applied the 3-D ray-based Kirchhoff prestack depth migration to generate migrated sections in single-layer homogeneous velocity models with orthorhombic anisotropy with and without the rotation of the tensor of elastic moduli.

In the case of *correct* orthorhombic anisotropy with the rotation of the tensor of elastic moduli around x_1, x_2 or x_3 axes, the migrated interface in the final stacked image coincides nearly perfectly with the interface in the model used to compute the recorded wave field. The distribution of elastic moduli in the *correct* model corresponds to the upper layer of the velocity model in which the corresponding synthetic data have been calculated.

In the case of *incorrect* orthorhombic anisotropy without the rotation of the tensor of elastic moduli, the errors of the migrated interface depend on the axis around which we rotate and on the rotation angle. The rotation around the axis x_1 caused that the migrated interface is shifted vertically upwards (undermigrated). When we rotated elasticity tensor around the axis x_2, one segment of the migrated interface is migrated correctly while other two segments are defocused and mispositioned (undermigrated). The rotation around the axis x_3 showed the smallest errors of the migrated interface. The migrated interface is slightly shifted vertically upwards (undermigrated). The errors of the migrated interface increase with the angle of the rotation for all rotation axes.

Acknowledgments

The author thanks Luděk Klimeš and Ivan Pšenčík for their help throughout the work on this paper.

The research has been supported by the Grant Agency of the Czech Republic under Contract P210/10/0736, by the Ministry of Education of the Czech Republic within Research Projects MSM0021620860 and CzechGeo/EPOS LM2010008, and by the members of the consortium "Seismic Waves in Complex 3-D Structures" (see "http://sw3d.cz").

References

Bucha, V. (2011): Kirchhoff prestack depth migration in 3-D models: Comparison of triclinic anisotropy with simpler anisotropies. In: *Seismic Waves in Complex 3-D Structures, Report 21*, pp. 47–62, Dep. Geophys., Charles Univ., Prague, online at "http://sw3d.cz".

Bucha, V. (2012a): Kirchhoff prestack depth migration in 3-D simple models: comparison of triclinic anisotropy with simpler anisotropies. *Stud. geophys. geod.*, **56**, 533–552.

Bucha, V. (2012b): Kirchhoff prestack depth migration in velocity models with and without gradients: Comparison of triclinic anisotropy with simpler anisotropies. In: *Seismic Waves in Complex 3-D Structures, Report 22*, pp. 29–40, Dep. Geophys., Charles Univ., Prague, online at "http://sw3d.cz".

Bucha, V. (2013a): Kirchhoff prestack depth migration in velocity models with and without vertical gradients: Comparison of triclinic anisotropy with simpler anisotropies. In: *Seismic Waves in Complex 3-D Structures, Report 23*, pp. 45–59, Dep. Geophys., Charles Univ., Prague, online at "http://sw3d.cz".

Bucha, V. (2013b): Kirchhoff prestack depth migration in velocity models with and without rotation of the tensor of elastic moduli: Poorly displayed part of migrated interface in correct model with triclinic anisotropy. In: *Seismic Waves in Complex 3-D Structures, Report 23*, pp. 61–69, Dep. Geophys., Charles Univ., Prague, online at "http://sw3d.cz".

Bucha, V. (2013c): Kirchhoff prestack depth migration in velocity models with and without rotation of the tensor of elastic moduli: Orthorhombic and triclinic anisotropy. In: *Seismic Waves in Complex 3-D Structures, Report 23*, pp. 71–80, Dep. Geophys., Charles Univ., Prague, online at "http://sw3d.cz".

Bulant, P. (1996): Two-point ray tracing in 3-D. *Pure appl. Geophys.*, **148**, 421-447.

Červený, V., Klimeš, L. & Pšenčík, I. (1988): Complete seismic-ray tracing in three-dimensional structures. In: Doornbos, D.J. (ed.), *Seismological Algorithms*, Academic Press, New York, pp. 89–168.

Gajewski, D. & Pšenčík, I. (1990): Vertical seismic profile synthetics by dynamic ray tracing in laterally varying layered anisotropic structures. *J. geophys. Res.*, **95B**, 11301–11315.

Schoenberg, M. & Helbig, K. (1997): Orthorhombic media: Modeling elastic wave behavior in a vertically fractured earth. *Geophysics*, **62**, 1954–1974.

Versteeg, R. J. & Grau, G. (eds.) (1991): *The Marmousi experience*. Proc. EAGE workshop on Practical Aspects of Seismic Data Inversion (Copenhagen, 1990), Eur. Assoc. Explor. Geophysicists, Zeist.